Low-Al tourmalines of 'oxy-dravite'–povondraite series from Cu–Au deposit of Ghagri area, Salumber–Ghatol belt, Aravalli Supergroup, Rajasthan

Fareeduddin[1,*], I. R. Kirmani[2] and Susmita Gupta[1]

[1]Geological Survey of India, PPOD Division, AMSE Wing, K.S. Layout, Bangalore 560 078, India
[2]Operations Rajasthan, Jhalana Dungari, Jaipur 302 004, India

Petrology and mineral chemistry of tourmalines from Cu–Au deposit in the Ghagri area, southeast Rajasthan are presented. The Cu–Au deposit is formed during the initial phase of Palaeoproterozoic Aravalli basin evolution with dominant deposition of shelf facies pelite-carbonate sequence of the Debari Group. This study suggests that the tourmalines possess a major povondraite component and follow an 'oxy-dravite'–povondraite crystallization trend. Extensive ultra-alkaline alterations, reported presence of scapolite-bearing assemblages, development of povondratic tourmalines and high Mg-bearing dravitic tourmalines with affinity to ultra-saline environments suggest that the tourmaline-bearing alteration zones in Cu–Au deposits of the Salumber–Ghatol belt have developed in an evaporitic environment.

Keywords: Cu–Au ore deposits, evaporites, hydrothermal, oxy-dravite, povondraite, tourmaline.

TOURMALINE, a common mineral in metal deposits of all kinds, is developed as a consequence of infiltration of boron-bearing hydrothermal fluids and can have a wide range of modal abundance (from accessory amounts to mono-mineralic layers called tourmalinites) and compositions that are representative of the bulk composition of the host lithologies and the invasive fluids[1]. It has a general formula[2], $XY_3Z_6(T_6O_{18})(BO_3)_3V_3W$ (where X = Ca, Na, K, vacancy; Y = Li, Mg, Fe^{2+}, Mn^{2+}, Zn, Al, Cr^{3+}, V^{3+}, Fe^{3+}, Ti $^{4+}$; Z = Mg, Al, Fe^{3+}, Cr^{3+}, V^{3+}; T = Si, Al, B; B = B, vacancy; V = OH, O, and W = OH, F, O). Fourteen species exist within the tourmaline group and the most common ones are elbaite, schorl and dravite. Among its mineral species the iron-rich and alumina-depleted end-member povondraite (studied earlier as 'ferridravite'[3]), with a crystal structure similar to buergerite has a chemical formula $NaFe^{3+}_3Fe^{3+}_6Si_6O_{18}(BO_3)_3$, $(O,OH)_4$ (ref. 4). 'Oxy-dravite' is the preliminary working name for a new member of the tourmaline group related to dravite by substitution on an OH by an O, the altered charge balance being compensated by replacing one Mg by a trivalent Al/Fe (its usual reference under quote implies that the new name awaits IMA approval). Hawthorne and Henry[2] showed that the ideal formula of povondraite is $NaFe^{3+}_3Mg_2Fe^{3+}_4Si_6O_{18}(BO3)_3$, $(O,OH)_4$ and that a solid-solution exists between povondraite of composition $NaFe^{3+}_3Mg_2Fe^{3+}_4Si_6O_{18}(BO3)_3$, $(O,OH)_4$ and 'oxy-dravite' $NaMgAl_2MgAl_5Si_6O_{18}(BO3)_3$, $(OH)_3O$. Povondraites and the intermediate members of the 'oxy-dravite'–povondraite series are rare[5–7]. In this article we report tourmalines that possess intermediate composition between 'oxy-dravite' and povondraite in an 'oxy-dravite'–povondraite series from a Cu–Au deposit of the Ghagri area in southeast Rajasthan and discuss the genesis of the deposit.

Geology

The Precambrian rocks, classified under Archaean (rocks older to ~2.5 b.y.) and Proterozoic (rocks formed between ~2.5 and 0.6 b.y.), occur in cratonic regions of the shield areas in all the continents. The Peninsular Indian Shield is a mosaic of cratonic regions of Dharwar, Bhandara–Bastar, Singhbhum, Bundelkhand and Aravalli, with their margins demarcated by shear zones and/or major fault systems. The cratonic regions are not only important for us to gain insight into the early history of the earth, but also because they constitute a storehouse of precious metal (Au, Ag), base-metal (Cu, Pb, Zn), ferrous metal (Fe, Mn) and rare metal (Pt, Pd, U, etc.) deposits.

The Aravalli craton in western India (Figure 1 *a*) is a repository of a variety of ore deposits (Pb, Zn, Cu, Au, W, Ag, U), which makes it one of the best metal provinces of India. The craton has recorded an uninterrupted Precambrian geological history (Figure 1 *a*) that manifested in the 3.3 b.y. (ref. 8). to 2.5 b.y. old (ref. 9) Archaean basement and two spectacular intersecting Proterozoic fold belts, viz. the older Palaeoproterozoic Aravalli fold belt and the younger Meso- to Neoproterozoic Delhi fold belt. Since Heron[10], various schemes of classification for

*For correspondence. (e-mail: fareedromani@hotmail.com)

the Proterozoic fold belts have been proposed[11,12]. The rocks of the Palaeoproterozoic Aravalli Supergroup occur in an inverted V-shaped basin towards the southeastern parts of the Aravalli Craton and are classified[11] into Debari, Udaipur and Jharol groups, each of which represents distinct depositional facies (with sparsely interspersed volcanic rocks, for example, Delwara volcanics in Debari Group). There is a paucity of absolute ages for the rocks of the Aravallli Supergroup. However, mention may be made of the basal Delwara volcanics that occur at the base of the Delwara Formation, and have yielded an age of ~2000 Ma (ref. 13) and U–Pb zircon ages of albite-rich rock from Bhukia area[14] that range between 1740 and 1820 Ma (ref. 14).

The 60 km long Salumber–Ghatol belt constituting the easternmost sector of the Aravalli Fold Belt in southeast Rajasthan exposes the rock sequences of the Debari Group. Shekhawat *et al.*[15] have classified these rocks into the lower Salumber Group and the upper Jaisamand Group, with the granitoids of the region being intrusive into the former and basement to the latter. The sequence has undergone polyphase deformation and a single metamorphic recrystallization event under green schist facies of metamorphism. This region is endowed with several Cu–Au deposits located at Bhukia, Ghagri, Dugocha, Hinglaz Mata, Timran Mata, Manpur, Kukra and Rajpura areas in structurally favourable loci[16,17].

The Ghagri area situated about 15 km east of Salumber, exposes thick polymictic conglomerate overlying basement gneisses (Banded Gneissic Complex) and, in turn, overlain by Delwara units that include mafic metavolcanics, dolomite and carbonaceous phyllite/chlorite schist and quartzites. The contact between dolomite and the mica-phyllite sequence is gradational. In the Cu–Au–Fe-oxide deposit area, mineralization occurs within dolomite with fairly extensive wall rocks manifested in the form of distal K-feldspathic (microclinites) rocks and proximal albitized dolomite rocks (ADR). The latter varies in thickness from less than a half a metre to about 20 m and invariably shows thickening and thinning feature (Figure 1 *b*). At times it is gritty in nature, consisting of fragments of chert, vein quartz and secondary carbonate encrustations. EPMA study has indicated that the feldspar in albite-carbonate rocks represents pure albite end-member and carbonates are distinctly dolomitic in composition (Table 1).

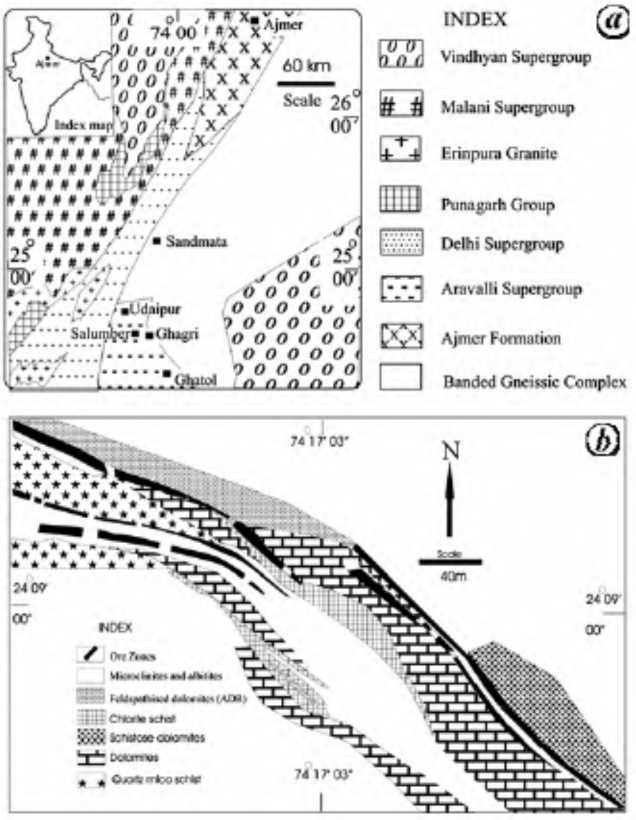

Figure 1. ***a***, Regional geological map of Rajasthan (simplified after Gupta *et al.*[11]; the Ajmer Formation shown is after Fareeduddin *et al.*[18]). ***b***, Detailed geological map of Ghagri Cu–Au prospect.

Tourmalines of Ghagri area

Tourmaline in the Ghagri Cu–Au deposit occurs in (i) massive sulphide horizons and (ii) in ADR. In sulphide-rich zones, two types of tourmaline occur, viz. (i) Sheaves and clusters of coarse prismatic purplish-brown tourmalines with interstitial albite and sulphides (Figure 2 *a* and *b*). They also form tourmalinite layers and lenses that are inter-fingered with the layers containing albite + carbonates and magnetite. (ii) Coarse-grained, euhedral, greenish, zoned tourmalines that occur in clusters with interstitial development of sulphides (Figure 2 *c*), maghematites, dolomites and rarely muscovites in semi-massive to sparsely sulphidic zones. These tourmalines are fractured, with fractures healed by sulphide ores. In ADR, the tourmalines occur as very fine size (10–50 μm), discrete, subhedral grains that constitute very fine, 2–6 mm size layers of tourmalinite that alternate with layers of albitite. The tourmalines in this unit also occur as simultaneously crystallized albite–tourmaline phases, wherein tourmaline occurs as anhedral patches within albites and also albite crystallizing as blebs within tourmalines.

EPMA study of the tourmalines (Table 1) indicates that the purplish tourmalines are poorer in alumina (average 24.99 wt%) then the green tourmaline (average 28.70 wt%). The tourmalines of ADR have moderate abundance level of alumina (average = 25.75 wt%). The purplish tourmalines are iron-rich (average FeO = 14.37 wt%, MgO = 7.03 wt%; $X_{Mg} = 0.47$), whereas the green tourmalines are Mg-rich (average FeO = 7.22 wt%, MgO = 8.81 wt%; $X_{Mg} = 0.7$). The tourmalines of ADR appear to be intermediate between the green and purplish tourmalines (average FeO = 12.58 wt%, MgO = 6.78 wt%; $X_{Mg} = 0.51$). In Ca–X-site vacancy–Na + (K) diagram (Figure 3 *a*) all

Table 1. Chemical analysis of tourmaline and other minerals from Ghaghri area[a,b]

	Sulphide-hosted purple tourmaline			Sulphide-hosted green tourmaline			ADR-hosted tourmaline					
	Minimum	Maximum	Average X = 8	Minimum	Maximum	Average X = 15	Minimum	Maximum	Average X = 5	Dolomite	Albite	Microcline
SiO_2	34.18	35.68	35.00	34.96	37.78	36.10	33.45	36.68	35.03	0.00	67.75	64.21
TiO_2	0.07	0.89	0.34	0.13	1.07	0.65	0.11	1.26	0.61	0.00	0.00	0.01
Al_2O_3	23.28	27.50	24.99	27.08	31.13	28.70	21.46	29.33	25.75	0.00	19.48	17.97
Cr_2O_3	0.00	0.06	0.01	0.00	0.11	0.03	0.00	0.04	0.01	0.00		0
FeO	11.97	17.08	14.37	5.25	10.44	7.22	7.64	18.47	12.58	1.06	0.81	0.06
MgO	6.79	7.24	7.03	7.70	9.89	8.81	5.98	7.76	6.78	22.37	0.00	0
CaO	0.47	0.93	0.74	0.13	0.48	0.32	0.06	0.88	0.47	31.60	0.01	0
MnO	0.00	0.07	0.04	0.00	0.06	0.02	0.00	0.15	0.08	0.62	0.00	0
BaO	0.00	0.06	0.01	0.00	0.25	0.05	0.00	0.28	0.10	0.02	0.00	0.26
Na_2O	2.28	2.58	2.46	2.52	2.96	2.70	2.32	2.85	2.58	0.00	11.68	0.27
K_2O	0.03	0.08	0.05	0.00	0.04	0.02	0.03	0.09	0.06	0.27	0.06	16.8
Total	83.70	85.91	85.02	82.69	87.44	84.51	82.88	84.52	83.84	55.94	99.79	99.58
H_2O[a]	3.37	3.53	3.44	3.48	3.75	3.58	3.28	3.58	3.43			
B_2O_3[a]	9.75	10.23	9.97	10.86	10.86	10.41	9.52	10.38	9.95			
Li_2O[a]	0.00	0.00	0.00	0.00	0.12	0.02	0.00	0.00	0.00			
Structural formula based on 31 anions (O, OH, F)[c]												
T : Si	6.06	6.14	6.11	5.94	6.13	6.05	6.08	6.15	6.12			
Al	0.00	0.00	0.00	0.00	0.06	0.01	0.00	0.00	0.00			
B	3.00	3.00	3.00	3.00	3.00	3.00	3.00	3.00	3.00			
Z : Al	4.84	5.51	5.14	5.49	5.90	5.67	4.62	5.82	5.29			
Mg	0.49	1.16	0.86	0.10	0.51	0.33	0.18	1.38	0.71			
Y : Ti	0.01	0.12	0.05	0.02	0.14	0.08	0.01	0.17	0.08			
Cr	0.00	0.01	0.00	0.00	0.02	0.00	0.00	0.01	0.00			
Mg	0.62	1.34	0.97	1.48	2.23	1.87	0.48	1.73	1.08			
Mn	0.00	0.01	0.01	0.00	0.01	0.00	0.00	0.02	0.01			
Fe^{2+}	1.70	2.52	2.10	0.70	1.48	1.01	1.07	2.79	1.86			
Zn	0.00	0.00	0.00	0.00	0.00	0.00	0.00	0.00	0.00			
Li*	0.00	0.00	0.00	0.00	0.08	0.01	0.00	0.00	0.00			
ΣY	3.03	3.18	3.11	2.88	3.06	2.97	2.77	3.30	3.01			
X : Ca	0.09	0.18	0.14	0.02	0.09	0.06	0.01	0.17	0.09			
Ba	0.00	0.00	0.00	0.00	0.02	0.00	0.00	0.02	0.01			
Na	0.78	0.87	0.83	0.84	0.92	0.88	0.81	0.93	0.87			
K	0.01	0.02	0.01	0.00	0.01	0.00	0.01	0.02	0.01			
X□	0.00	0.07	0.03	0.02	0.09	0.06	0.00	0.07	0.03			
CatSum	19.08	19.29	19.20	18.90	19.05	18.97	18.89	19.38	19.10			
XMg	0.41	0.52	0.47	0.65	0.77	0.70	0.37	0.64	0.51			

[a]Full analysis available with the authors and would be provided upon request.
[b]Analysed using CAMECA SX100 Electron Microprobe at GSI, Bangalore.
[c]Calculated using Andy Trindle Free Software developed by Julie Selan and Jim Xiang, freely available on the internet.

the tourmalines of this area plots in the field of alkali group tourmalines near the Na + (K) end. The alkaline nature of the tourmalines is further confirmed by their X-site, which is dominated by Na (purplish tourmaline – 0.78–0.87 apfu; green tourmaline – 0.84–0.92 apfu; ADR – 0.81–0.93 apfu). All the tourmalines are Al-deficient (< 6 apfu) and when the data are plotted on an Al–Fe–Mg ternary diagram (Figure 3 *b* and *c*), it can be seen that all types of tourmaline from the Ghagri area have Al content that falls below the dravite–schorl join and plot in the field of Fe^{3+}-rich quartz tourmaline rocks, calc-silicates and metapelites. The most significant feature of the tourmaline chemistry is that they plot along the 'oxy-dravite'–povondraite join (Figure 3 *c*).

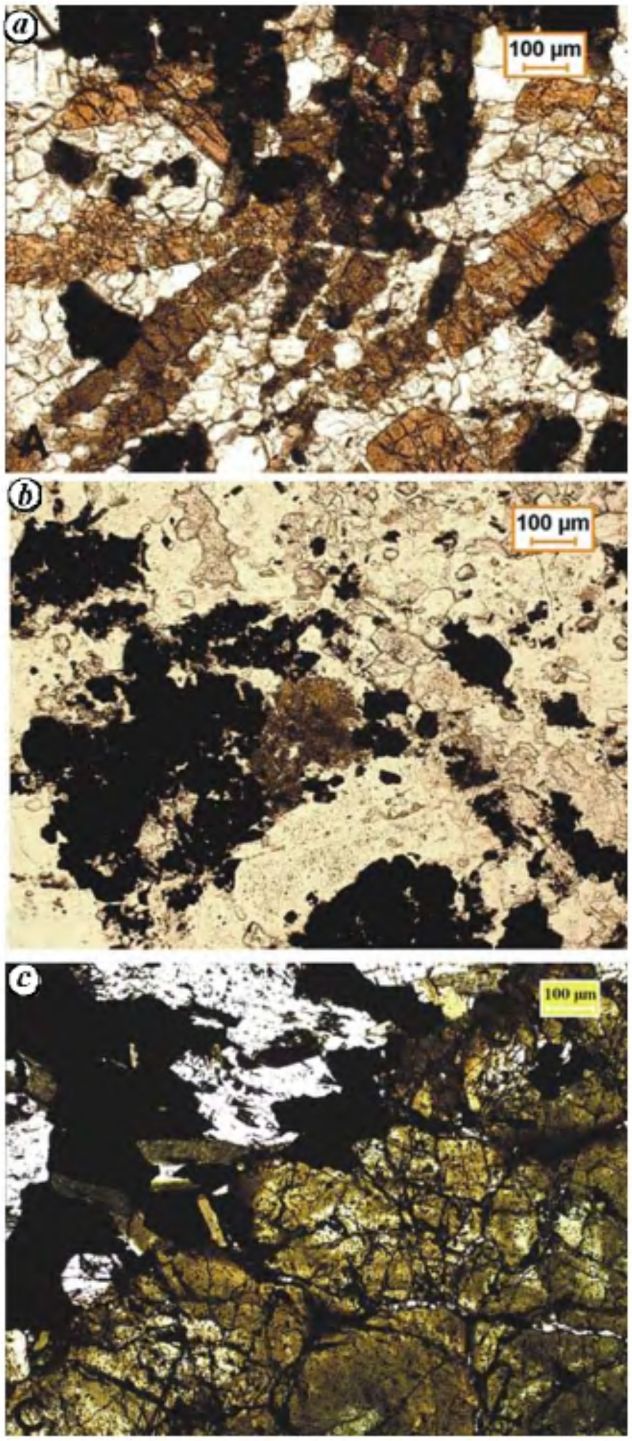

Figure 2. Photomicrographs showing (*a*) prismatic plates of purplish tourmalines in groundmass of dolomite and albite, plane polarized light (PPL); (*b*) Intergrowth of purplish tourmalines, with sulphides (dark). The other minerals present are dolomite (turbid) and albite (white), PPL; (*c*), Zoned green tourmaline developed in sulphide-rich zones. Note that the euhedral tourmalines are intensely fractured and the fractures are healed with the sulphides, PPL.

Henry *et al.*[7] have devised a series of diagrams that show important site substitutions and the influence of different exchange vectors in tourmalines. In Mg–Ca versus Fe diagram (Figure 4 *a*), the Ghagri tourmaline data plot along a line that represent dravite–schorl join and are parallel to MgFe-1 exchange vector. In Al + Ca versus Fe diagram (Figure 4 *b*), two distinct clusters are observed for purplish and green tourmalines with ADR tourmalines getting distributed in both clusters, but when taken together the Ghagri tourmalines distinctly define a dominant MgFe-1 exchange vector. Henry *et al.*[7] have demonstrated that the Al versus Fe subsystem can be isolated by accounting for the influences of other constituents, such as Mg, Ca, Ti and X-site vacancies, through projection of the exchange vectors that most likely introduce these constituents. This type of representation results in the dravite and schorl end-members being projected to the same point along the 'oxy-dravite'–povondraite join. An implication is that tourmaline having Al–X-site vacancy + Ca values that plot along this join, but significantly less than that of the dravite/schorl projected point, is most strongly influenced by FeAl-1 exchange. Conversely, tourmaline with Al–X-site vacancy + Ca values along this join but significantly greater than the dravite/schorl projected point, is mainly influenced by AlO(R(OH))-1 exchange. In Al–X-site vacancy + Ca versus R + X-site vacancy – Ca + Ti diagram (Figure 4 *c*) the tourmaline data in general array parallel to the 'oxy-dravite'–povondraite join, but the distribution of the two major types of tourmaline appears to be different in that the purplish tourmalines plot above the dravite/schorl projected point, and therefore must have been influenced by FeAl-1 exchange. On the other hand, the green tourmalines plot below the dravite/schorl projected point and are strongly influenced by AlO(R(OH))-1 exchange.

These plots indicate that: (i) the Ghagri tourmalines in general are characterized by MgFe-1 exchange vector, but when the Al versus Fe subsystem can be isolated by accounting for influences of other constituents, such as Mg, Ca, Ti and X-site vacancies, the distinction between the two types of tourmaline becomes more apparent, with purplish and green tourmalines showing the influence of FeAl-1 and AlO(R(OH))-1 exchange vectors respectively; (ii) these tourmalines plot close or parallel to the 'oxy-dravite'–povondraite join and therefore represent mineral species belonging to this solid solution series. Higher

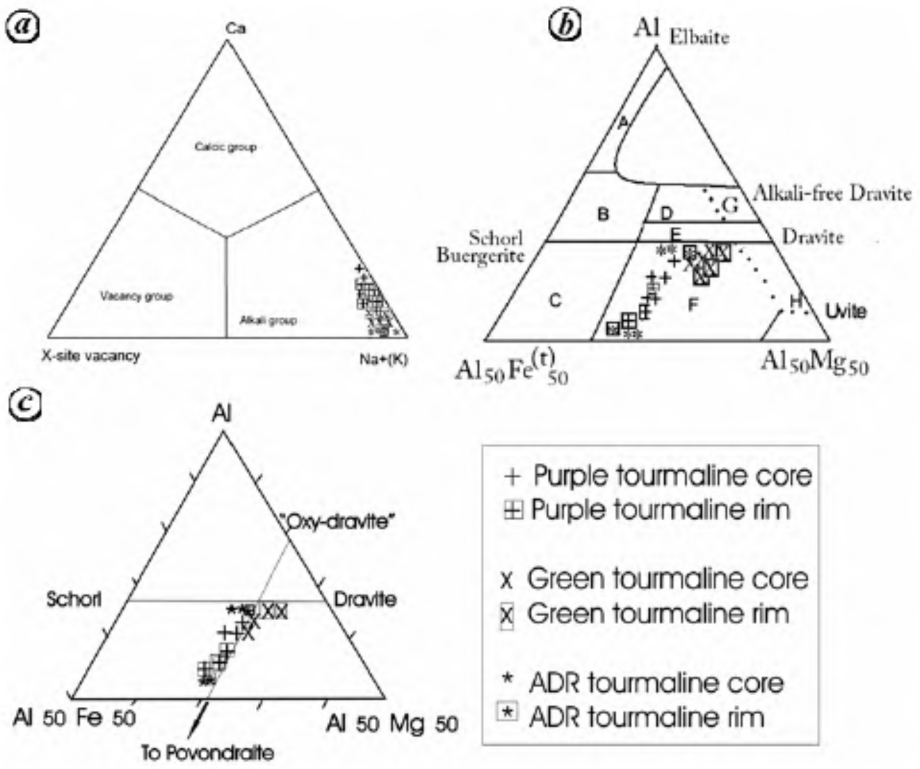

Figure 3. ***a***, Ca–X-site vacancy-Na + K diagram (after Hawthorne and Henry[2]) for core and margin chemistry of tourmalines from the area under study. Note that all the tourmaline analyses fall within the alkali-group field. ***b***, Al–$Fe^{(tot)}$-Mg diagram (after Henry and Guidotti[22]) for tourmalines from Ghagri area. Different regions in the diagram represent compositional range of tourmalines from different sources. (A) Li-rich granitoid, pegmatities and aplites; (B) Li-poor granitoids, pegmatites and aplites; (C) Fe^{3+}-rich quartz–tourmaline rocks (hydrothermally altered granites); (D) Metapelites and metapsammites co-existing with an Al-saturating phase; (E) Metapelites and metapsammites not co-existing with Al-saturating phase; (F) Fe^{3+}-rich quartz–tourmaline rocks, calc-silicates and metapelites; (G) Low-Ca metaultramafics and Cr, V-rich metasediments and (H) Metacarbonates and metapyroxinites. ***c***, Al–Fe–Mg diagram showing 'oxydravite'–povondraite trend for tourmalines of the Ghagri area.

concentration of Fe^{3+} places the tourmaline closer to 'oxy-dravite' than povondraite in this series.

Discussion

Tourmaline chemistry is a sensitive indicator of the environment in which its mineral species crystallize. The Ghagri tourmalines are alkali-rich, with Na being the dominant alkali element present and with tourmalines having small amounts of X-site vacancy. This composition is consistent with tourmalines in equilibrium with an aqueous fluid enriched in Na with albite[7,18]. The 'oxy-dravite'–povondraite tourmalines have Mg of ~2.0 apfu, typically have O_2 as the dominant occupant of the W site, and exhibit chemical variations in accordance with the FeAl-1 and/or AlO(Fe(OH))-1 exchange vectors[7]. In Ghagri area all the tourmalines are significantly deficient in Al (<6 apfu), consistent with a dominance of FeAl-1 exchange. These features together are consistent with an environment of formation that was relatively oxidizing with a low H_2O activity such as a saline environment. Tourmalines with similar composition are reported from evaporate-bearing assemblages of Alto Chapare, Bolivia, Challenger knolls, Gulf of Mexico and Liaoning, China[5–7].

The occurrence of povondratic tourmaline in mineralized zones of Cu–Au deposit of Ghagri area has some important implications for the models proposed for the origin of such deposits. The two commonly quoted and intensely argued[19,20] sources of fluids for Cu–Au ± iron-oxide deposits include: (i) magmatic–hydrothermal source and (ii) non-magmatic evaporitic source. The magmatic model requires an alkali-rich magmatic source that accounts for subordinate Fe-oxide and relatively large Na (± K) alterations. The evaporitic model requires surface-derived or basin-derived fluids which mingle with igneous-derived solutes that flow along a large-scale plumbing system and manifest in the form of extensive albitic and related alteration zones. Significant mineralogical and geochemical inhomogeneity would be expected in the non-magmatic system than in the magmatic system. The evaporitic model explains sufficiently enormous volumes of sodic alterations normally associated with this kind of deposit. Such sodic alterations are pervasive in this 70 km long Salumber–Ghatol belt. This evidence together with the presence of high Mg-dravite and scapolite-bearing

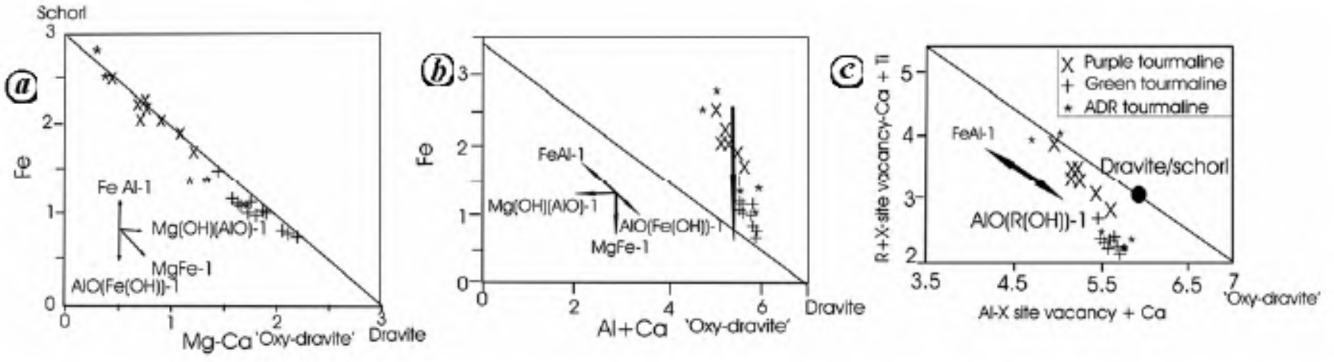

Figure 4. Binary diagrams (after Henry *et al.*[7]) showing different exchange vectors in Ghagri tourmaline. ***a***, Mg–Ca versus Fe; ***b***, Al + Ca versus Fe; ***c***, Al–X-site vacancy + Ca versus R + X-site vacancy – Ca + Ti diagram.

assemblages associated with mineralization at Bhukia[21] advocate for an evaporitic source model for the formation of Cu–Au-bearing horizons of this region. Occurrence of 'oxy-dravite'–povondaritic tourmalines in Ghagri Cu–Au mineralized zones further supports an evaporitic source for the metal-rich alkali and boron-bearing fluids of the Salumber–Ghatol belt.

1. Slack, J. F., Tourmaline associations with hydrothermal ore deposits. In *Boron: Mineralogy, Petrology and Geochemistry* (eds Grew, E. S. and Anovitz, A. M.), Rev. Minerals, 1996, pp. 559–640.
2. Hawthorne, F. C. and Henry, D. J., Classification of the minerals of the tourmaline group. *Eur. J. Mineral.*, 1999, **11**, 201–215.
3. Walenta, K. and Dunn, P. J., Ferridravite, a new mineral of the tourmaline group from Bolivia. *Am. Mineral.*, 1997, **64**, 945–948.
4. Grice, J. D., Ercit, T. S. and Hawthorne, F. C., Povendraite, a redefinition of the tourmaline ferridravite. *Am. Mineral.*, 1993, **78**, 433–436.
5. Zacek, V., Fryda, A., Petro, A. and Hyrdl, J., Tourmalines of povondraite–(oxy)dravite – series from the cap rock of metaevaporite in Alto Chapare, Cochabamba, Bolivia. *J. Czech. Geol. Soc.*, 2000, **54**, 3–12.
6. Basik, P., Uher, P., Sykora, M. and Lipka, J., Low-Al tourmalines of the schorl–dravite–povondraite series in redeposited tourmalines from the western Carpathians, Slovakia. *Can. Minerol.*, 2008, **46**, 1117–1130.
7. Henry, D. J., Sun, H., Slack, J. F. and Dutrow, B. L., Tourmalinites from metaevaporites and highly magnesian rocks: perspective from Namibian tourmalinites. *Eur. J. Mineral.*, 2008, **20**, 889–904.
8. Gopalan, K., Macdougall, J. D., Roy, A. B. and Murali, A. V., Sm–Nd evidence for 3.3 Ga old rocks in Rajasthan, northwestern India. *Precambrian Res.*, 1990, **48**, 287–297.
9. Choudhury, A. K., Gopalan, K. and Sastry, C. A., Present status of the geochronology of Precambrian rocks of Rajasthan. *Tectonophysics*, 1984, **105**, 131–140.
10. Heron, A. M., Geology of Central Rajputana. *Mem. Geol. Surv. India*, 1953, **79**, 389.
11. Gupta, S. N., Arora, Y. K., Mathur, R. K., Iqbaluddin, Prasad, B., Sahai, T. N. and Sharma, B., The Precambrian geology of the Aravalli Region, Southern Rajasthan and Northwestern Gujarat. *Mem. Geol. Surv. India*, 1997, **123**, 262.
12. Roy, A. B., Stratigraphic and tectonic framework of the Aravalli Mountain Range. In *Precambrian of Aravalli Mountain Range, Rajasthan, India* (ed. Roy, A. B.), Memoirs of the Geological Society of India, 1988, No. 7, pp. 3–31.
13. Deb, M. and Thorpe, R. I. (eds), Geochronological constraints in the Precambrian geology of Rajasthan and their metallogenic implications. In *Sediment-hosted Lead–Zinc Sulfides with Emphasis on the Deposits in the Northwestern Indian Shield*, Narosa Publishing House, New Delhi, 2004, pp. 246–263.
14. Deb, M., Some key issues of gold metallogeny in India. In International Workshop on Gold Metallogeny in India, Delhi University, Abstrt., 2008, pp. 50–53.
15. Shekhawat, L. S., Joshi, D. W. and Pandit, M. K., A re-look into the status of granitoids and conglomerate in Salumber–Jaisamand area, southern Rajasthan: Implication for the stratigraphy of the Palaeoproterozoic Aravalli Fold Belt. *J. Geol. Soc. India*, 2001, **58**, 53–63.
16. Grover, A. K. and Verma, R. G., Gold mineralisation in the Precambrian (Bhukia area) of southeastern Rajasthan – a new discovery. *J. Geol. Soc. India*, 1993, **42**, 281–288.
17. Fareeduddin, Kirmani, I. R. and Davay, D. R., Gold in sulfide ores of Rajasthan – a review. *Indian Mineral*, 1995, **50**, 369–376.
18. Fareeduddin, Reddy, M. S. and Bose, U., Reappraisal of the Delhi stratigraphy in Ajmer–Sambhar sector. *J. Geol. Soc. India*, 1995, **45**, 667–679.
19. Lynch, G. and Ortega, J., Hydrothermal alteration and tourmaline–albite equilibria at Coxheath porphyry Cu–Mo–Au deposit, Nova Scotia. *Can. Mineral.*, 1997, **35**, 79–94.
20. Barton, M. D. and Johnson, D. A., Evaporitic-source model for igneous-related Fe-oxide–(REE–Cu–Au–U) mineralization. *Geology*, 1996, **24**, 259–262.
21. Golani, P. R., Pandit, M. K., Sial, A. N., Fallick, A. E., Ferreira, V. P. and Roy, A. B., B–Na rich Palaeoproterozoic Aravalli metasediments of evaporitic association, NW India: a new repository of gold mineralization. *Precambrian Res.*, 2002, **116**, 183–198.
22. Henry, D. J. A. and Guidotti, C. V., Tourmalines as a petrogenetic indicator mineral: an example from the staurolite-grade metapelites of NW Maine. *Am. Mineral.*, 1985, **70**, 1–15.

ACKNOWLEDGEMENTS. We thank the Deputy Director General, Geological Survey of India (GSI), Bangalore for permission to publish this paper. We also thank Drs S. P. Venkata Dasu, J. N. Das and R. Anantharayana, GSI, for encouragement and Basab Chattopadhyay, N. C. Pant and Shyamal Sengupta (GSI) for help in EPMA analytical work.

Received 15 October 2009; revised accepted 3 September 2010